Identifying key design parameters of the integrated energy system for a residential Zero Emission Building in Norway

Authors: Natasa Nord[1*], Live Holmedal Qvistgaard[2], Guangyu Cao[1]

Affiliations:

[1]Norwegian University of Science and Technology (NTNU), Department of Energy and Process Engineering, NO-7491 Trondheim, Norway

[2]Norconsult AS, Norway

[*]E-mail address: natasa.nord@ntnu.no. Phone number: (+47) 73593338.

Abstract

This study examined an integrated solution of the building energy supply system consisting of flat plate solar thermal collectors in combination with a ground-source heat pump and an exhaust air heat pump for the heating and cooling, and production of domestic hot water. The supply energy system was proposed to a 202 m^2 single-family demo dwelling (SFD), which is defined by the Norwegian Zero Emission Building standard. The main design parameters were analyzed in order to find the most essential parameters, which could significantly influenced the total energy use. This study found that 85 % of the total heating demand of the SFD was covered by renewable energy. The results showed that the solar energy generated by the system could cover 85-92 % and 12-70 % of the domestic hot water demand in summer and winter respectively. In addition, the solar energy may cover 2.5-100 % of the space heating demand. The results showed that the supply air volume, supply air and zone set point temperatures, auxiliary electrical volume, volume of the DHW tank, orientation and tilt angle and the collector area could influenced mostly the total energy use.

Keywords: zero emission building, renewable energy, ground source heat pump, exhaust air heat pump, family house

1. Introduction

The annual energy demand in the building sector in Norway represents about 40 % of the total national energy use, of which 22 % goes to residential sector and 18 % to the non-residential sector [1]. In residential buildings, space heating (SH) and domestic hot water (DHW) represent approximately 70 % of the total energy use [2]. The building sector therefore has the great potential to obtain higher energy savings nationwide. Predictions indicate that the Norwegian energy use for residential purposes will be reduced by 75 % in 40 years from now on. In 2010, a recast of the Energy Performance of Buildings Directive (EPBD) was adopted by the European Parliament and the Council of the European Union, which states that by 2020 new buildings in the EU will have to use 'nearly zero' energy and the energy will be 'to a very large extent' from renewable sources [3]. The development of energy systems that improve the integration between renewable energy sources and thermal requirements, while guaranteeing a comfortable indoor climate is crucial.

Earlier studies have defined methods to calculate the energy use in a ZEB [4, 5]. A building may be characterized as a ZEB when it is able to export excess energy, generated by photovoltaic (PV) modules for instance, to the grid and achieve an annual net balance between demand and supply. In Norway, the minimum requirements of energy efficiency for a ZEB single-family dwelling are stated in the standard describing the requirements for passive houses and low energy buildings [6]. Passive residential buildings are characterized by an enhanced building envelope, where the consequence is reduced specific design power demand (W/m^2), reduced annual specific energy demand ($kWh/m^2 \cdot year$), and an increased share of annual heat demand for DHW. In passive residential buildings for instance, the hot water demand represents 40 – 85 % of total annual heating demand [7]. Developing sustainable solutions for DHW systems based on solar energy is therefore highly relevant.

In Norway, the sun provides 1 500 times more energy than what is used [8]. The annual solar irradiation in Norway varies from 700 kWh/m^2 in the north to 1100 kWh/m^2 in

the south due to different latitudes. It has been calculated that solar heating systems will be able to cover 60 % of the DHW demand and 30 % of the SH demand in all new residential buildings for a year. This means that the theoretical potential for solar heating by 2020 is 65 GWh/year for SH and 131 GWh/year for DHW for new residential buildings of passive house standard [9]. Developing an integrated solution which may use the excess heat collected by solar collector and thereby utilize the full potential of the solar thermal technology becomes important. There are a few solutions that can be used to overcome heat imbalance problem. For example, by tilting the solar collectors a larger share of the solar irradiation can be collected [10]. Thermal energy storages (TES) must be carefully matched to each specific application, and the selection of a TES system is highly dependent on storage period, economic viability, and operating conditions [11]. For a heating system with a combination of solar collectors and a ground-source heat pump (GSHP) it is relevant to look into the borehole TES technology for storing. Combining solar collectors with a GSHP has been increasingly recognized in Europe since the oil crises in the 1970s, but the technology has not been widely adopted [12].

However, there are few studies on developing an integrated heating system for single-family dwellings (SFDs) are relatively scarce, especially in Norway. Integrated solar energy systems, which provide both DHW and space heating (solar combi-systems), may result in a diverse range of different designs that may reflect local climate and practice [13]. Even though seasonal storage of solar heat in boreholes for detached houses is not widely examined, theoretical calculations show that charging the borehole with solar heat is beneficial [14]. Incorporating the ground-source heating system with supplementary components, such as thermal solar collectors, can improve the imbalance which occurs in the soil due to thermal heat depletion. An experimental study of a heating system which combined GSHP and thermal solar collectors showed that the COP of the heat pump gradually decreased as the heating season advanced. When the excess solar heat was injected

into the boreholes consequently, the operational conditions of the system was improved and COP of the heat pump was increased [12]. Chiasson and Yavuzturk performed an assessment of the viability of a GSHP coupled with solar thermal collector (STCs) in heating dominated buildings. This study shows that combining solar collectors with a GSHP reduced the borehole length at the design with a reduction per solar collector area ranging from 4.5 (Omaha, Nebraska) to 7.7 m/m^2 solar collector area (Cheyenne, Wyoming) [15]. Compared to conventional solar heating systems, the energy system where the excess heat can be used to recharge the boreholes or a swimming pool promotes a longer operational time for the solar collectors. During the winter time the solar radiation is limited and only low temperatures can be reached in the solar collectors. Even though the heat collected by the solar collectors is insufficient for DHW or space heating, the produced solar heat can be used to recharge the borehole. This may increase the borehole temperature and may provide the heat pump with better operational conditions [16].

As the building envelope will become tighter due to the implementation of the new building code in Norway, there has been a growing interest in using mechanical ventilation systems with exhaust air heat pumps (EAHP) as heat recovery in the Nordic European countries [17]. The EAHP utilizes the exhaust air in a balanced ventilation system as heat source, and is able to provide heat for DHW, supply air, and SH. For instance, a heat pump may generate 60-70°C water if the ambient air is 24°C than if it is 1.7°C [18].

In this study, the design of the integrated renewable energy supply system was analyzed in the SFD in Larvik, Norway, which is one of the most favorable locations in Norway for utilization of solar energy. The main feature of this building was that the majority of the energy demand should be covered by renewable energy sources available on site. The SFD was called the “Multikomfort” and is a demo project conducted by the Norwegian Research Centre on Zero Emission Buildings (ZEB) and a partner company.

The objective of this study was to examine the essential design parameters for the integrated energy system of a ZEB family house in the cold climate. The novelty of this study is a thorough analysis of a complex energy supply system based on the renewable energies.

2. Methods

Relevant information regarding the energy supply for the ZEB dwelling were collected from the ZEB project [19]. The input for ventilation system, constructions, internal loads, and DHW demand was set in accordance with NS 3700 – Criteria for passive houses and low energy buildings – Residential buildings [6]. In order to investigate the system performance and total energy use the dynamic simulation tool IDA-ICE was used. The mathematical models are described in terms of equations in a formal language. IDA-ICE performs a whole-year detailed and dynamic multi-zone simulation, which enables analysis of the thermal indoor climate and the energy consumption of the entire building. In IDA-ICE, a standard plant or an Early Stage Building-Optimization plant (ESBO-plant) can be chosen as energy supply plant. The ESBO-plant enables the opportunity to select among different renewable energy sources and then build the plant accordingly. Further it is possible to modify the plant as desired. With the possibility of using the ESBO-plant, IDA-ICE is able to simulate the complex energy supply system for a SFD "Multikomfort".

Design improvement can be performed by sensitivity analysis and optimization. Many studies have been dealing with parametric and sensitivity analysis by using Monte Carlo method [20, 21] or ready-to-use tools, such as SIMLAB, [22]. Optimization of building performance can be performed by using specifically developed tools, such as GenOpt, [23, 24] or by coupling building performance simulation tools with MATLAB [25, 26]. However, due to the smoothness problem of the building simulation models built in the simulation tools, it is difficult to analyze and perform a detail analysis of huge number of parameters [27]. Specifically, the problem becomes complex when the building model is complex. Therefore,

many studies developed rather a simple building model and perform complex optimization and sensitivity analysis. In this study, a very complex building model with the STC in combination with a GSHP and an EAHP, which was additionally added in IDA-ICE, was developed. A complex sensitivity analysis or optimization was difficult to be performed immediately. Therefore, the idea was to exanimate firstly the most important design variables as a preparation for the further studies. By comparing the relative change in the electricity use for each of relevant design parameter, the parameters with the greatest impact can be identified as

$$k = \frac{\Delta E}{\Delta X} \cdot 100\ \% \quad (1)$$

where ΔE is the percentage change in electricity use and ΔX is the percentage change in the observed parameter.

3. ZEB demo building

3.1. Building model

The building investigated in this study is located in Larvik in Norway as a demonstration ZEB building, which was designed as a SFD according to the Zero Emission Building definition with the ambition level ZEB-O&M (Operation and Material). The SFD was designed to accommodate a family of four to five members with related outdoor area. A model of the building is shown in Figure 1.

The SFD is a two-story family home with a floor area of 202 m^2. The ground floor consists of an entrance, bathroom, media room, office, living room and kitchen. The first floor accommodates a bathroom, hall, and three bedrooms. The roof has a slope of 19°, and is equipped with PV-panels and STCs as integrated parts of the roof construction. Electricity production from the PV-panels was not analyzed in this study. The ventilation system was a balanced, mechanical ventilation system with constant air flows. The volume flow rate was 240 m^3/h. Compared to the floor plans in the real building, some simplifications were made

in IDA-ICE in order to reduce the simulation time. For instance, the open space from the ground floor to the first floor with the staircase was not implemented. The bedrooms and hallway on the first floor were simulated as one zone and the ground floor was divided into two zones, one zone representing the kitchen, bathroom and hall, and one zone for the living room and office/bedroom.

Figure 1. Architecture view of the SFD "Multikomfort"

U-values for the external walls, the roof, and the external floor were set in accordance with the requirements stated in NS 3700 [6]. The U-values and the normalized thermal bridge values are given in Table 1. The total U-value of the windows was calculated to be 0.63 W/m^2K.

Table 1. U-values and normalized thermal bridge value according to NS 3700 [6]

3.2. Energy supply system

The analyzed energy supply system is shown in Figure 2, which consists of a GSHP, STCs, and an EAHP. The excess solar heat was only utilized to recharge the borehole. The EAHP supplied thermal energy to the DHW storage tank; and cooperates with solar energy in order to preheat DHW. The ventilation air was heated directly from the ground-source heat exchanger.

The flat plate solar collectors were used in the system. The tilt angle of collectors should be 19° facing the south-east. The heat-transfer fluid is a 33 % mixture of glycol-water. The brine to water GSHP had a heating rate of 3 kW and a COP of 4.6 as given in the heat pump documentation. The condenser heating rate of the EAHP was set to 1.2 kW and the COP was set to 3.9, which corresponded to the data from the heat pump. Only one borehole with a depth of 80 m was included. Finally, the analyzed energy supply system modelled in

IDA-ICE consisted of three main circuits: the solar water circuit, the GSHP circuit, and the EAHP circuit. The annual average temperature in Larvik is 6.3°C. Based on the standard requirements [6], the annual specific heating demand for the demo house was calculated to be 17.6 kWh/m^2, which was slightly above the German requirement of 15 kWh/m^2.

Figure 2. Energy supply system with solar thermal system, GSHP, and EAHP

The energy supply system (shown in Figure 2) would be utilized in combination with a low-temperature floor heating system. The temperature of the supply and return water of the heat distribution system were 35/30°C. The whole system could be divided into six modules, including the solar collector subsystem, the DHW supply subsystem, the closed loop ground-source subsystem, the ventilation system, the GSHP subsystem and the space heating subsystem. Basic design parameters are listed in Table 2.

Table 2. Basic system design parameters

3.3. Occupants' behavior and design parameters

In order to achieve realistic operation conditions for the STCs, a correct schedule for the use of the DHW was defined as shown in Figure 3. DHW draw-off for a single-family house usually has some peaks during the morning and the evening.

Figure 3. Distribution of DHW usage

The heat contribution from equipment, lighting, and persons were calculated according to recommended values stated in NS 3700. The values for equipment and lighting in each zone are listed in Table 3.

Table 3. Internal loads, equipment and lighting

The specific heating load for the floor heating in each zone is given in Table 4.

Table 4. Heating rate and specific design heating load

The ventilation system was a central air handling unit with balanced and constant air flow rates. The total airflow rate in the air handling unit was set to 240 m^3/h with a supply temperature of 19°C all the year. According to the NS 3031the minimum specific airflow rate for a dwelling with floor area above 110 m^2 is 1.2 $m^3/h \cdot m^2$ [28]. An airflow rate of 240 m^3/h is in accordance with the requirement defined by the partner company. The airflow rates supplied to different rooms are given in Table 5.

Table 5. Supply and exhaust air flow rates

4. Results and discussions

The energy supply system illustrated in Figure 2 with some simplifications together with the dwelling in Figure 1 was simulated in IDA-ICE 4.6 with a solar collector area of 16 m^2 and floor heating as heating system in the dwelling. With an oversized solar collector area, excess solar heat could be utilized to recharge the borehole during the summer months.

4.1. System performance

The distribution of the collected solar heat between the DHW tank, the SH tank, and the borehole through the year is shown in Figure 4. Solar heat was transferred from the SH tank to the DHW tank from January to November of the year 2013, and the highest heat input was found during the summer months. Approximately 300 kWh was transferred to the DHW tank in June. Since the circulation pump between the STC and the water storage tank was not in operation when the temperatures near the bottom of the tank exceeds 60°C due to the control setting, excess solar heat was transferred to the ground. The borehole was recharged

with solar heat from April to September, and the highest heat input was found from May to August, which was expected. Approximately 600 kWh of solar heat was transferred to the ground in July, which was twice as much as the heat transferred to the DHW tank in the same month. By increasing the control setting of 60°C, more solar heat would probably be utilized for DHW production instead of recharging the borehole. However, when increasing the temperature set point at the bottom of the DHW tank, the temperature at the top of the tank may exceed its maximum allowable temperature. By comparing the results it was proven that recharging the borehole with excess solar heat resulted in a slight increase in evaporator brine inlet temperature from April to October. Due to the increase in brine inlet temperature, a slight increase in the GSHP COP was observed as well. Transferring solar heat to the SH tank was the second priority in the solar heating system. As seen in Figure 4, solar heat was transferred to the SH tank during the heating season. The highest solar heat input was found in March and April, and approximately 100 kWh of solar energy was transferred to the SH tank in these months. It can be seen that solar heat is also utilized for space heating in September and October.

Figure 4. Heat flow from solar circuit to DHW tank, SH Tank and to ground

Figure 5 shows the temperature of entering brine evaporator and the temperature from the GSHP to the SH tank. The dark green line represents the entering evaporator temperature from the ground, while the lighter green represents the leaving condenser temperature from the GSHP. The temperature rise from the evaporator to the condenser was approximately 30-40°C. A gap in temperature is registered about 3000-6000 hours, which is during the summer season. In this period, the GSHP was turned off since there was no heating demand, and the temperatures were therefore relatively irregular. The temperature entering the SH tank lied between 35 and 45°C, which is sufficient to meet the SH temperature requirement of 35°C.

Figure 5. Entering and leaving brine water of the GSHP

Figure 6 shows the compressor energy use, the condenser energy, and the energy gained from the ground through the year. It shows that the GSHP was not in operation during the summer months when there was no heating demand. The COP was dependent on the condenser heat rate and the compressor power. When the share of compressor power constituted a larger part of the condenser power, the COP decreased. The condenser heat rate varied through the year depending on the demand and the temperatures in the tank, and thus the compressor power and the COP varied as well. The COP varied between 3.5 and 4.5, which was considered to be sufficient.

Figure 6. Annual performance of GSHP

Figure 7 shows the annual performance of the EAHP. The energy demand of exhaust air was reduced towards the summer months. From January to June, the demand was reduced with approximately 50 %, which indicates that a greater proportion of the DHW demand was covered by the solar heat in the summer.

Figure 7. Annual performance EAHP

In order to determine the thermal performance of the system, the annual solar fraction was calculated. The solar fraction is defined as the energy supplied by the solar part of the system divided by the total system load [29], and was calculated as:

$$Annual\ solar\ fraction = \frac{Net\ utilized\ solar\ energy}{Total\ heating\ demand} \quad (2)$$

Figure 8 shows the total delivered energy of the energy system. The "Electrical heating" column represents the electrical energy utilized by the electrical boilers, and the compressors in both the GSHP and the EAHP. HVAC Aux covers the electricity use of the fans and pumps in the system. The annual total specific delivered energy for the SFD is 35.5 kWh/m^2.

Figure 8. Delivered energy

Figure 9 shows the monthly energy balance between the energy demand and the amount of utilized renewable energy. Both the SH demand and the DHW demand were included in the "Energy demand" columns. The obtained monthly solar fractions are represented by the orange line, and the solar fractions was 100 % from May to August . This indicated that excess solar heat is produced. The system's total annual solar fraction for the simulated year was 35.9 %. The specific heating demand for the SFD was 27.1 kWh/m^2, which was higher than the required 17.6 kWh/m^2 stated in NS 3700.

Figure 9. Energy demand, utilized free energy and solar fraction

4.2. Effects of the design parameters

Effects of the most important design parameters on the ZEB dwelling energy use are presented. The values of the parameters which have been elucidated and utilized in the study are based on information and recommendations found in the literature. During the simulations, only one parameter was changed at a time, while all other parameters in the system were kept at initial settings. However, it was still difficult to get close to how the system performance would be in reality due to the complex nature of combi-systems [30]. Initially the reference system had a solar collector area of 16 m^2. As the system performance

311 and system electricity use would be affected by the area of the solar collector, solar collector
312 areas between 8 and 16 m^2 were investigated.

313 Figure 10 shows the total monthly solar fraction for each different solar collector area.
314 The solar fractions presented the total system's solar fraction and includes the solar energy
315 utilized to recharge the borehole. The results showed that the highest monthly solar fractions
316 were obtained with a solar collector area of 16 m^2. The difference in solar fraction between
317 16, 14 and 12 m^2 of solar collector area was however not particularly large, and excess solar
318 heat was produced from May to July. The solar fraction was reduced by 7 % and 8 % in
319 March and April respectively, by decreasing the collector area from 16 to 14 m^2. The
320 reduction in solar fraction in September and October was 6 % and 5 %. During the summer
321 months, approximately 50 and 60 % of the DHW demand was covered by solar energy with
322 solar collector areas of 14 and 16 m^2. With a collector area of 8 m^2, 45-50 % of the DHW
323 demand was covered by solar energy from May to August.
324
325 Figure 10. Monthly solar fractions for different solar collector areas

326 Table 6 shows the total annual solar fraction and the total annual electricity use for
327 each solar collector area.
328
329 Table 6. Annual solar fraction and specific delivered energy for different solar collector areas
330
331 Figure 11 shows the system's annual solar fraction and the annual specific delivered
332 energy for tilt angles of 19°, 40°, 55° and 60° with an orientation towards the south. By
333 orientating the solar collectors with a tilt angle of 19° towards the south instead, the annual
334 solar fraction was increased by 11 % and the specific delivered energy was decreased by 1.1
335 %. By increasing the tilt angle to 40° and 55°, the annual solar fraction is increased by 17.0 %
336 and 18.0 % respectively. A decrease in annual solar fraction occurred when the angle was

changed from 55° to 60°, which indicated that a tilt angle of 55° results in a better system performance.

Figure 11. Annual solar fraction and annual specific delivered energy - south orientation

Assuming a consumption of 100-150 l/day resulted in a total DHW tank volume of 100-300 liters. The SH tank volume was approximately 100-200 l per kW heating load. For the “Multikomfort”, a space heating of 2.8 kW was used, which resulted in a tank volume of approximately 280-560 liters. Figure 12 shows the total annual solar fraction and the specific delivered energy affected by the difference in DHW tank volume. It can be seen that by increasing the tank volume, the thermal performance of the system is increased accordingly. Additionally, a larger tank volume resulted in diminished effect from the other heat sources on the solar volume and a lower temperature was maintained at the lower part of the tank. This resulted in decreased inlet temperatures to the solar collectors, which increased the collector efficiency. A decrease of 3-4 K in inlet collector temperature was observed when increasing the tank volume from 180 l to 300 l. The annual solar fraction was increased by approximately 3 % and the specific delivered energy is decreased by 3.7 % by increasing the tank volume from 180 l to 300 l.

Figure 12. Annual solar fraction as a function of the volume of the DHW tank

Figure 13 shows the annual solar fraction and the specific delivered energy for the SH tank as a function of the storage tank volume. Increasing the height/diameter (h/d)-ratio of the tank further had no significant effect on the system performance. A dependency between the annual solar fraction and the h/d ratio was however observed. By reducing the h/d-ratio to 1.5 the annual solar fraction was decreased by 0.6 %, and by increasing the h/d-ratio to 2.6, the

363 increase in annual solar fraction was 0.3 % compared to the initial h/d-ratio of 2.08. The
364 specific delivered energy was not affected by the change in h/d-ratio.
365
366 Figure 13. Annual solar fraction and specific delivered energy as a function of SH tank
367 volume

368 By comparing Figure 12 and Figure 13, it shows that changing the DHW storage tank
369 volume had a greater effect on the annual solar fraction. So storing solar energy in the SH
370 tank might be the second priority in the system. The effect on the annual solar fraction and
371 specific delivered energy in the SH tank was not as striking as for the DHW tank. The annual
372 solar fraction has a very gentle slope from a volume of 325 l to 500 l, and that the specific
373 delivered energy was constant. It shows that a SH tank volume of 560 l was insufficient since
374 a noticeable increase in specific delivered energy was obtained. In addition, increasing the
375 tank volume to 560 l resulted in a higher heat loss to the surroundings, and as a consequence
376 more electricity is used to cover the space heating demand.

377 Table 7 shows annual solar fraction and specific delivered energy with borehole
378 diameters ranging from 11–16 cm were performed. The initial borehole diameter is 11.5 cm.
379 The amount of net utilized solar energy was the only result affected by the change in borehole
380 diameter. By increasing the diameter from the original setting of 11.5 cm to 15.5 cm the net
381 utilized solar energy increases by 3.3 kWh/a, which only constitutes a minor difference and
382 may be regarded as negligible.
383
384 Table 7. Annual solar fraction and specific delivered energy for each borehole diameter
385

386 The supply air flow rate in the dwelling is initially based on the minimum permitted
387 average air volume flow rate stated in NS 3031, which is 1.2 $m^3/h \cdot m^2$. Figure 14 shows the
388 annual specific delivered energy, as well as the annual average CO_2-concentration registered
389 in the dwelling. The electrical energy use was considerably reduced when the air volume flow

rate was decreased (see Figure 14). It can be seen that the CO_2-concentration increases as the supply air flow rate decreased as expected. The CO_2-concentration presented in Figure 14 was the total CO_2-concentration and included the outdoor concentration, which was assumed to be 350-400 ppm in Norway [31]. For dwellings classified as the indoor air quality class 1 (highest), the indoor CO_2-concentration should not exceed 350 ppm above outdoor concentration. Indoor air quality class 2 (medium) requires the CO_2-concentration should not exceed 500 ppm above outdoor concentration. The general recommendation in Norway is a total CO_2-concentration below 1000 ppm in order to secure sufficient indoor air quality. In order to have an acceptable air quality, it is recommended that the supply air flow rate is 7 l/s per person in the respective room [31]. This roughly coincides with a volume flow rate of 1.2 $m^3/h \cdot m^2$. Figure 14 shows that the average CO_2-concentration never exceeded 1000 ppm. However, on a daily basis the registered CO_2-concentration is higher, and with a volume flow rate of 0.9 $m^3/h \cdot m^2$, concentrations higher than 1000 ppm were found. As the volume flow rate decreased, the local age-of-air in each room increased and the air might be perceived as "heavy" and uncomfortable.

Figure 14. Annual specific delivered energy as a function of air volume flow rate

The set supply water temperature in the SH system was initially set to 35°C, which ensures that the heating demand is met at all the time. The supply temperatures ranging from 28–35°C were simulated, while all other parameters were kept at the initial settings. Table 8 shows that by decreasing the supply temperature, the specific delivered energy decreased. Decreasing the supply temperature to 30°C resulted in 700 hours of unmet heating. Several days in the winter months have temperatures below 19°C, which was considered to be too low. With a supply temperature of 32°C, the lowest indoor air temperature occurred in a day in January, which was 19.6°C, which was considered acceptable. The specific delivered

energy was reduced by 0.8 % when the supply air temperature was decreased from 35 to 32°C. By decreasing the supply temperature from 35 to 32°C, an increase in GSHP COP was observed, which enhanced the system performance.

Table 8. Specific delivered energy with different heating system supply temperatures

4.3. Defining the key design parameters

In Figure 15 the change in utilized electrical energy, ΔE, is shown in %. Figure 15 shows the examined parameters with the greatest impact on the electricity use of the whole system. The results provided an indication for designers what parameters should be focused on in order to optimize the performance of the system. The column representing the change of solar collector area was derived from the difference in installing a suitable collector area of approximately 8 m^2 to an oversized collector area of 16 m^2. The column which represents the auxiliary electrical volume in the DHW tank was derived from the difference in using an auxiliary volume of 100 l, which is recommended in the literature, and an auxiliary volume of 50 l. Figure 15 provides evident that an efficient storage tank design was crucial as well as the orientation and tilt angle of the solar collectors. With an oversized solar collector area, approximately 1.6 % of the electricity use could be saved. Approximately 3.6 % of electrical energy could be saved by reducing the supply air and zone set point temperature from 20°C to 19°C. It can be seen that the supply air volume flow rate has a great impact on ΔE. Approximately 4.2 % of the electricity use is decreased just by reducing the supply air flow rate from 1.2 to 1.0 $m^3/h \cdot m^2$ floor area.

Figure 15. Design parameters which gave the greatest reduction in electricity use

Table 9 shows the relative change of each parameters in these simulations. It was found that the supply air volume, supply air and zone set point temperatures had the greatest impact on the system's electricity use when taking the percentage change into account. The relative change obtained for the DHW tank volume and solar collector area are rather small, due to the percentage change in parameter. When the change results in increased component size, the amount of energy saved must be evaluated in context with the cost of installing enhanced solar collectors or larger storage tanks, for instance. A large change in parameter accompanied with a small change in saved energy may be regarded as unprofitable.

Table 9. Relative change in parameter, k

If the implemented analysis method together with the integrated energy supply system would be applied to a different building model, a similar trend as in Figure **15** in the electricity use would be noted due to changes of supply air volume, supply air, and zone set point temperatures. Regarding the borehole depth, the trend might be different than in Figure **15** for different buildings.

5. Conclusions

In this study, an integrated energy supply system for the SFD was analyzed, where the combination of the STC, the GSHP, and the EAHP was included. The combination of the STC and GSHP made it possible to alleviate many of the disadvantages which appeared if a solar collector heating system or a GSHP system operates separately. The study showed that reducing the supply airflow rate and decreasing the set point of supply air temperature and zonal temperature resulted in a notable decrease in electricity use. This conclusion might be similar for different buildings, too. However, in the case of the borehole depth, the conclusions might be different for the different buildings.

By introducing the possibility to store solar energy in a borehole from summer to winter, the COP of the heat pump might be increased. However, only one borehole for the SFD was needed and recharging the borehole with excess solar heat might be unnecessary due to fast natural recovery. The results from the simulations showed that by recharging the borehole with excess solar heat during the summer months, a slight increase in the GSHP COP was obtained from April to October. However, the increase had minor impact on the performance of the heat pump and thereby the total system's electricity use. Recharging the borehole was beneficial as it protected the solar collectors from overheating, in the long run it might lead to overheating of the ground which results in reduced possibility to utilize free cooling. For a SFD it might be more efficient to utilize the excess solar heat for other purposes, e.g. heating of a swimming pool.

The study showed that the design of the short time storage tank was crucial as well as the tilt angle and orientation of the solar collectors. Tilting and orientating the solar collectors towards the recommended directions might reduce the heat loss of 4 %. It could also be concluded that only half the solar collector area was needed as long as the tilt angle and orientation were proper in order to obtain the same system performance. Optimizing the tilt angle and orientation would influence the possibility of using the solar collector area as part of the roof construction and the benefit must be considered in coherence with the cost of the extra roof construction. The main issues impeding the utilization of renewable energy sources for SH and heating of DHW might be the development of economically competitive and reliable means for seasonal storage of thermal energy.

Acknowledgment

This work has been supported by the Research Council of Norway and partners through the research projects "*The Research Centre on Zero Emission Buildings*". ZEB is one of several Norwegian national Centers for Environment-friendly Energy Research. The

493 authors are also thankful to company Brødrene Dahl, for sharing information about their
494 demo project.

495

496 **References**

497

498 [1] I. Sartori, B.J. Wachenfeldt, A.G. Hestnes, Energy demand in the Norwegian building stock:
499 Scenarios on potential reduction. Energy Policy, 2009. 37(5): p. 1614-1627.
500 [2] Norwegian Water Resources and Energy Directorate, Energy use. 2011 [cited 2013; Available
501 from: http://www.nve.no/Global/Publikasjoner/Publikasjoner%202011/Rapport%202011/rapport9-
502 11.pdf.
503 [3] Energy Performance of Buildings Directive, Directive 2010/31/EU, European Council for an
504 Energy Efficient Economy, 2010.
505 [4] J. Kurnitski, A. Saari, T. Kalamees, M. Vuolle, J. Niemelä, T. Tark, Cost optimal and nearly zero
506 (nZEB) energy performance calculations for residential buildings with REHVA definition for nZEB
507 national implementation. Energy and Buildings, 2011. 43(11): p. 3279-3288.
508 [5] A.J. Marszal, P. Heiselberg, J.S. Bourrelle, E. Musall, K. Voss, I. Sartori, A. Napolitano, Zero
509 Energy Building – A review of definitions and calculation methodologies. Energy and Buildings,
510 2011. 43(4): p. 971-979.
511 [6] NS3700 - Criteria for passive houses and low energy buildings. Residential buildings, Standards
512 Norway, 2013.
513 [7] J. Stene, Heating systems for housing of low energy and passive standard, Sintef Energy Research,
514 A4606, 2008,
515 [8] I. Andresen, Planning of solar heating for low-energy and passive houses -an introduction, Sintef
516 Building and Infrastructure, 2008.
517 [9] U.M. Halvorsen, P. Bernhard, F. Salvesen, L. Bugge, I. Andresen, S. I, Feasibility study of solar
518 energy in Norway, Sintef Building and Infrastructure and KanEnergi, 2011.
519 [10] E. Kjellsson, Solar Collectors Combined with Ground-Source Heat Pumps in Dwellings.
520 Analyses of System Performance, PhD thesis, Lund University, 2009.
521 [11] G.K. Pavlov, B.W. Olesen, Thermal energy storage-A review of concepts and systems for heating
522 and cooling applications in buildings: Part 1-Seasonal storage in the ground. HVAC and R Research,
523 2012. 18(3): p. 515-538.
524 [12] V. Trillat-Berdal, B. Souyri, G. Fraisse, Experimental study of a ground-coupled heat pump
525 combined with thermal solar collectors. Energy and Buildings, 2006. 38(12): p. 1477-1484.
526 [13] W.W. Weiss, Solar heating systems for houses: a design handbook for solar combisystems, 2003,
527 London: James & James. xii, 313 s., [16] s. of plates : ill. (some col.). 9781601197115

[14] R.K. Ramstad, E-mail correspondence regarding solar seasonal storage in boreholes, 2013: Trondheim, Norway.
[15] A.D. Chiasson, C. Yavuzturk, Assessment of the Viability of Hybrid Geothermal Heat Pump Systems with Solar Thermal Collectors, ASHRAE Transations 109, 2003.
[16] E. Kjellsson, G. Hellström, P. Bengt, Optimization of systems with the combination of ground-source heat pump and solar collectors in dwellings, Energy, 2010, 35(6): p. 2667-2673.
[17] D. Sakellari, P. Lundqvist, Energy analysis of a low-temperature heat pump heating system in a single-family house, International Journal of Energy Research, 2004, 28 (1): p. 1-12.
[18] A. Hepbasli, Y. Kalinci, A review of heat pump water heating systems, Renewable and Sustainable Energy Reviews, 2009, 13 (6-7): p. 1211-1229.
[19] ZEB, *About The Research Centre on Zero Emission Buildings - ZEB*, www.zeb.no, 2013.
[20] T.D. Pettersen, Variation of energy consumption in dwellings due to climate, building and inhabitants. Energy and Buildings, 1994. 21(3): p. 209-218.
[21] M. Kavgic, A. Summerfield, D. Mumovic, Z. Stevanovic, Application of a Monte Carlo model to predict space heating energy use of Belgrade's housing stock. Journal of Building Performance Simulation, 2014.
[22] H. Breesch, A. Janssens, Performance evaluation of passive cooling in office buildings based on uncertainty and sensitivity analysis. Solar Energy, 2010. 84(8): p. 1453-1467.
[23] N. Djuric, V. Novakovic, J. Holst, Z. Mitrovic, Optimization of energy consumption in buildings with hydronic heating systems considering thermal comfort by use of computer-based tools. Energy and Buildings, 2007. 39(4): p. 471-477.
[24] N. Djuric, Real-time supervision of building HVAC system performance, PhD thesis in Department of Energy and Process Technology, 2008, Norwegian University of Science and Technology: Trondheim. p. 224.
[25] M. Hamdy, A. Hasan, K. Siren, Applying a multi-objective optimization approach for Design of low-emission cost-effective dwellings. Building and Environment, 2011. 46(1): p. 109-123.
[26] M. Hamdy, A. Hasan, K. Siren, A multi-stage optimization method for cost-optimal and nearly-zero-energy building solutions in line with the EPBD-recast 2010. Energy and Buildings, 2013. 56: p. 189-203.
[27] M. Wetter, BuildOpt - A new building energy simulation program that is built on smooth models. Building and Environment, 2005. 40(8): p. 1085-1092.
[28] NS 3031, Calculation of energy performances of buildings, Method and data, Standards Norway, 2007.
[29] EN9488, Solar energy Vocabulary, European committee for standardization, 1999.
[30] W. Weiss, Solar heating systems for houses - a design handbook for solar combisystems, 2003, London: James & James.
[31] V. Novakovic, S.O. Hanssen, J.V. Thue, I. Wangensten, F.O. Gjerstad, ENØK i bygninger: effektiv energibruk, 2007, Oslo: Gyldendal undervisning. 476 s. : ill. ; 27 cm. 978-82-05-37496-6

567

Tables

Table 1. U-values and normalized thermal bridge value according to NS 3700:2013

	Values
External walls	U = 0.10-0.12 W/m²K
External roof	U = 0.08-0.09 W/m²K
Slab on ground	U = 0.07 W/m²K
Windows	U = 0.65 W/m²K
Doors	U = 0.65 W/m²K
Normalized thermal bridge value	Ψ = 0.03 W/m²K

Table 2. Basic system design parameters

Site location: Larvik (lat. N59°03, long.E10°02)			
Indoor/outdoor winter design temperatures	21°C/-17°C		
Borehole number	1		
Borehole depth	80 m		
Brine/water GSHP	**COP**		**Heating capacity**
	4.6		3 kW
Solar collector	**Collector area**		**Efficiency**
	8m²/16m²		60 %
Exhaust air heat pump	**Air/air**		**Air/water**
COP	4.6		3.9
Heating capacity	2.0 kW		1.2 kW
DHW tank	**Volume**	**Electrical supply**	**Heat loss coefficient**
	180 l	1.5 kW	-
Storage tank for space heating	**Volume**	**Electrical supply**	**Heat loss coefficient**
	325 l	3.0 kW	2.0 kWh/day

Table 3. Internal loads, equipment and lighting

	Equipment	Lighting
NS 3700:2013	1.80 W/m²	1.95 W/m²
Kitchen/hallway	138 W	150 W
Living room/office	91 W	100 W
Bedrooms	138 W	150 W

Table 4. Heating rate and specific design heating load

Zone	Floor area [m²]	Heating rate [W]	Design heating load [W/m²]
1st floor, bedrooms	75.7	1174	16
Living room/office	50.6	1041	21
Kitchen/hallway	75.7	1006	13

Table 5. Supply and exhaust air flow rates

	Supply Air flow rate	Exhaust air flow rate [m^3/h]	Comment
Kitchen/hall	90 m^3/h	90 m^3/h	
Bedrooms	90 m^3/h	90 m^3/h	
Living room/office	60 m^3/h	60 m^3/h	
Total	**240 m^3/h**	**240 m^3/h**	**Gives 1.2 [m^3/hm^2]**

Table 6. Annual solar fraction and specific delivered energy for different solar collector areas

	16 m^2	14 m^2	12 m^2	10 m^2	8 m^2
Total annual solar fraction [%]	35.9	32.8	29.5	25.9	22.3
Total annual specific delivered energy [kWh/m^2]	35.5	35.6	35.7	35.9	36.1

Table 7. Annual solar fraction and specific delivered energy for each borehole diameter

	11.5 cm	12.5 cm	13.5 cm	14.5 cm	15.5 cm
Net utilized solar energy [kWh/a]	4183.5	4184.2	4184.7	4185.0	4186.8
Specific delivered energy [kWh/m^2]	35.5	35.5	35.5	35.5	35.5

Table 8. Specific delivered energy with different heating system supply temperatures

Supply temperature heating system	**28°C**	**30°C**	**32°C**	**35°C (initial setting)**
Specific delivered energy [kWh/m^2]	34.9	35.1	35.2	35.5

Table 9. Relative change in parameter, k

	Supply air volume	Supply temperature	Auxiliary volume	DHW tank volume	Collector area
Relative change [%]	25.2	38.5	4.6	5.5	1.7

Figure 1

Click here to download high resolution image

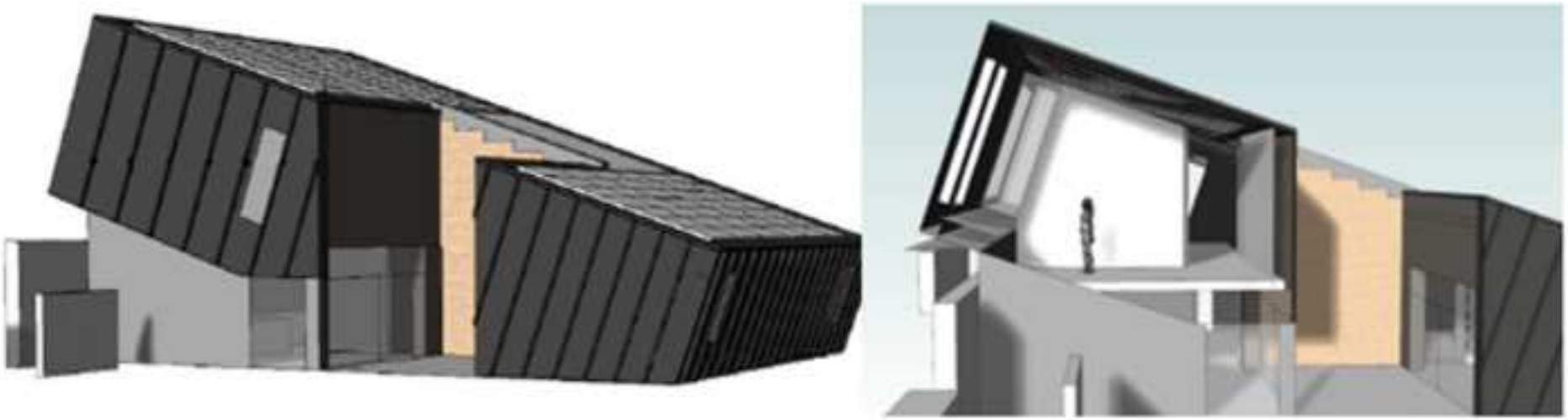

Figure 2

Click here to download high resolution image

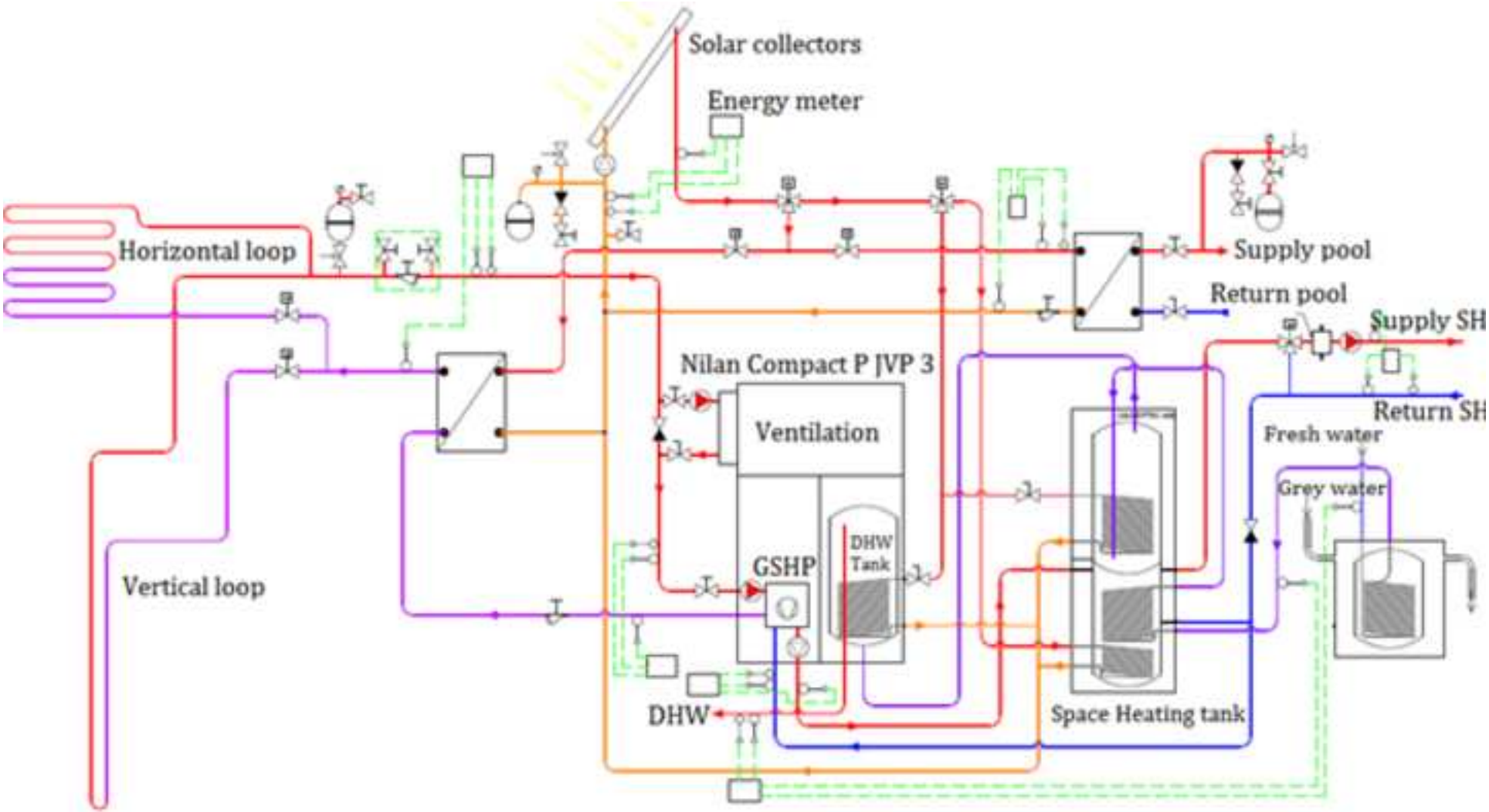

Figure 3

Click here to download high resolution image

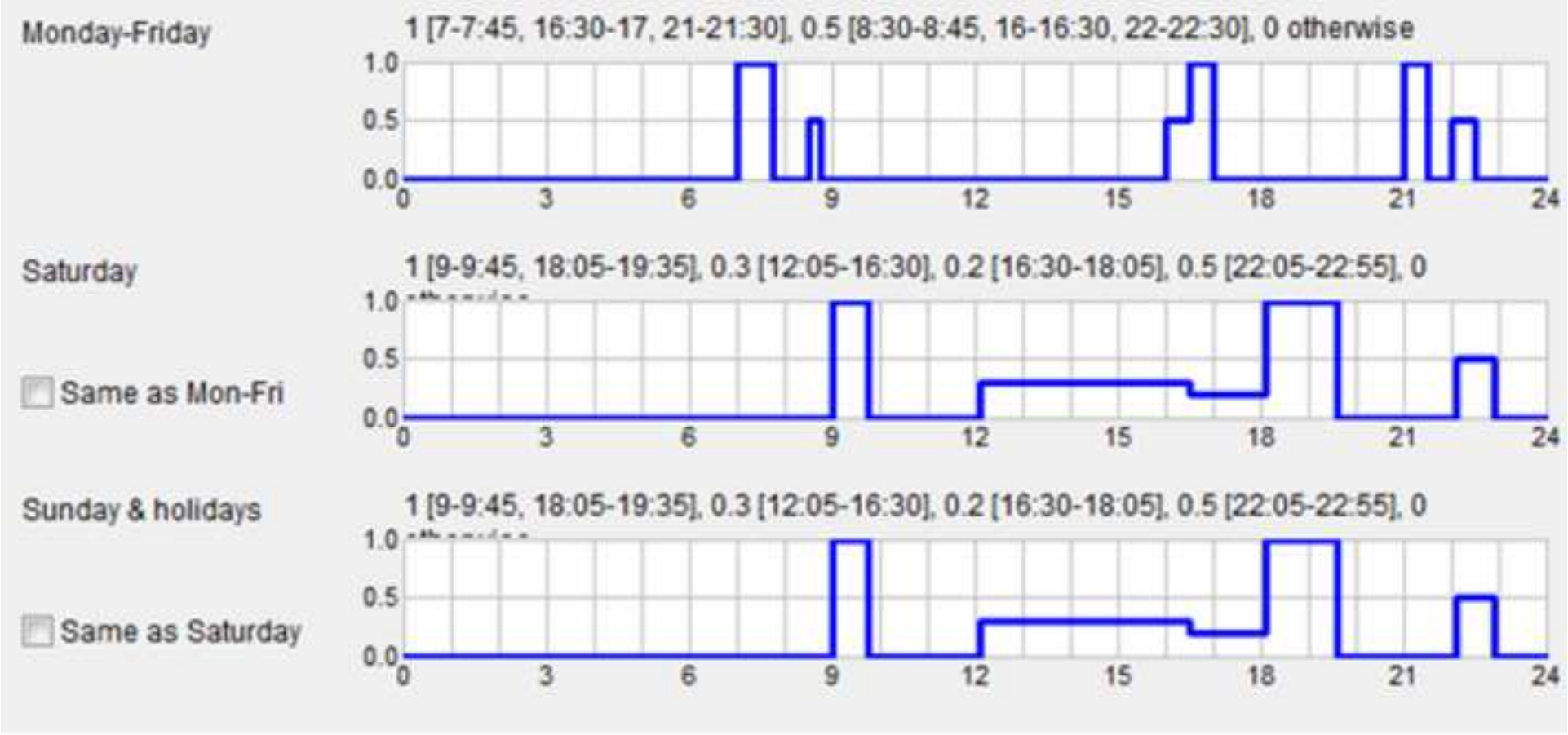

Figure 4

Click here to download high resolution image

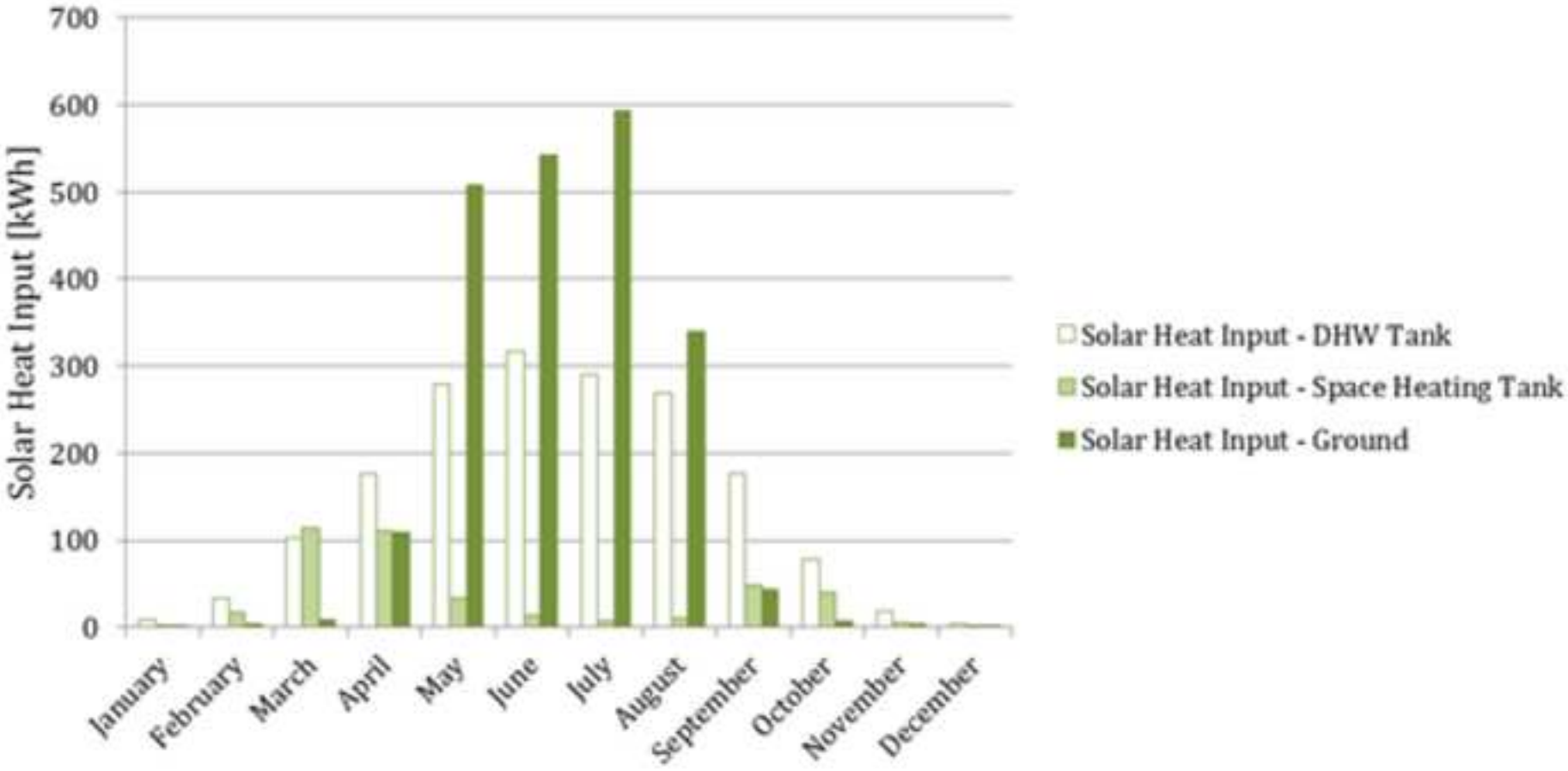

Figure 5

Click here to download high resolution image

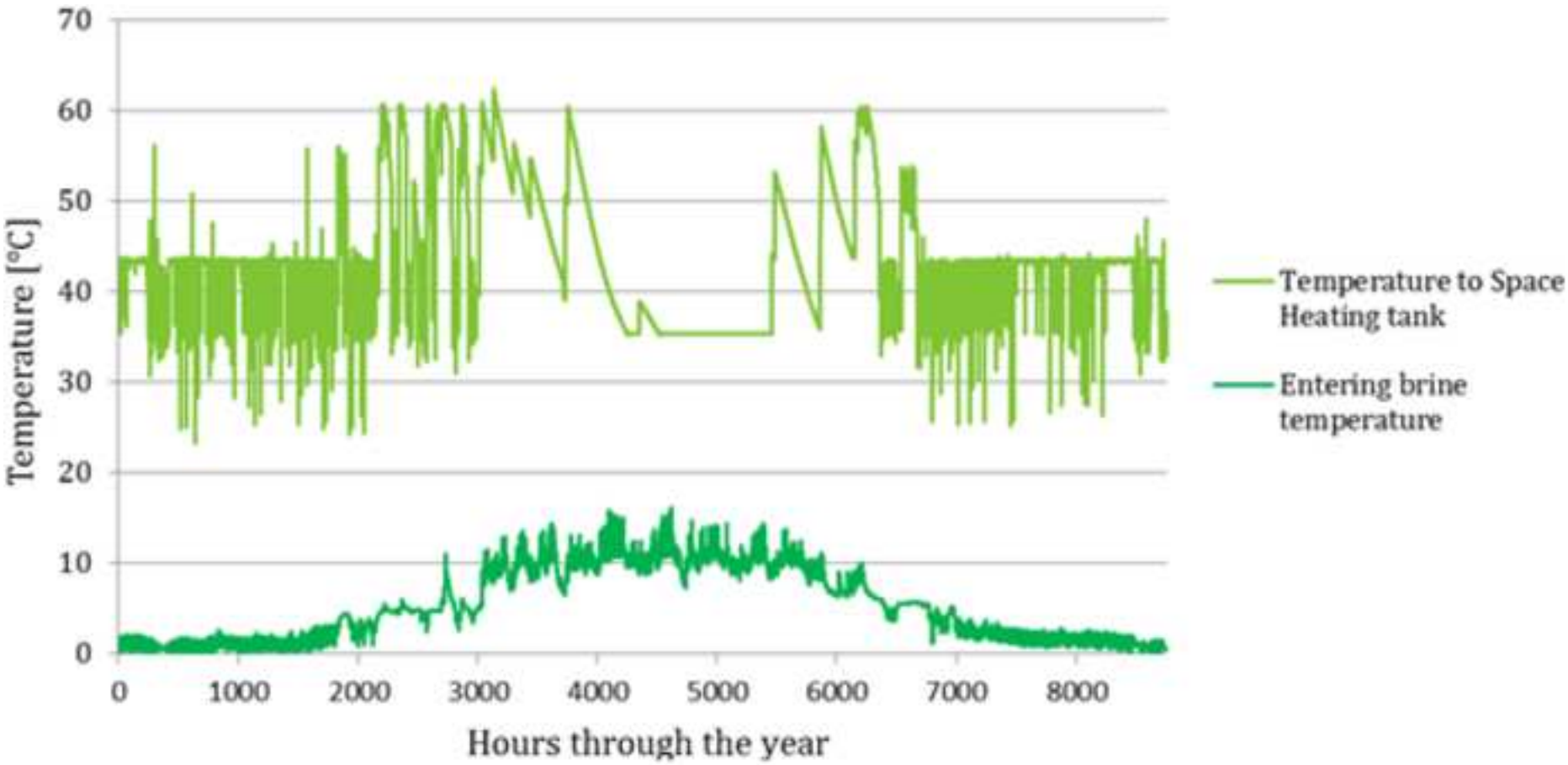

Figure 6

Click here to download high resolution image

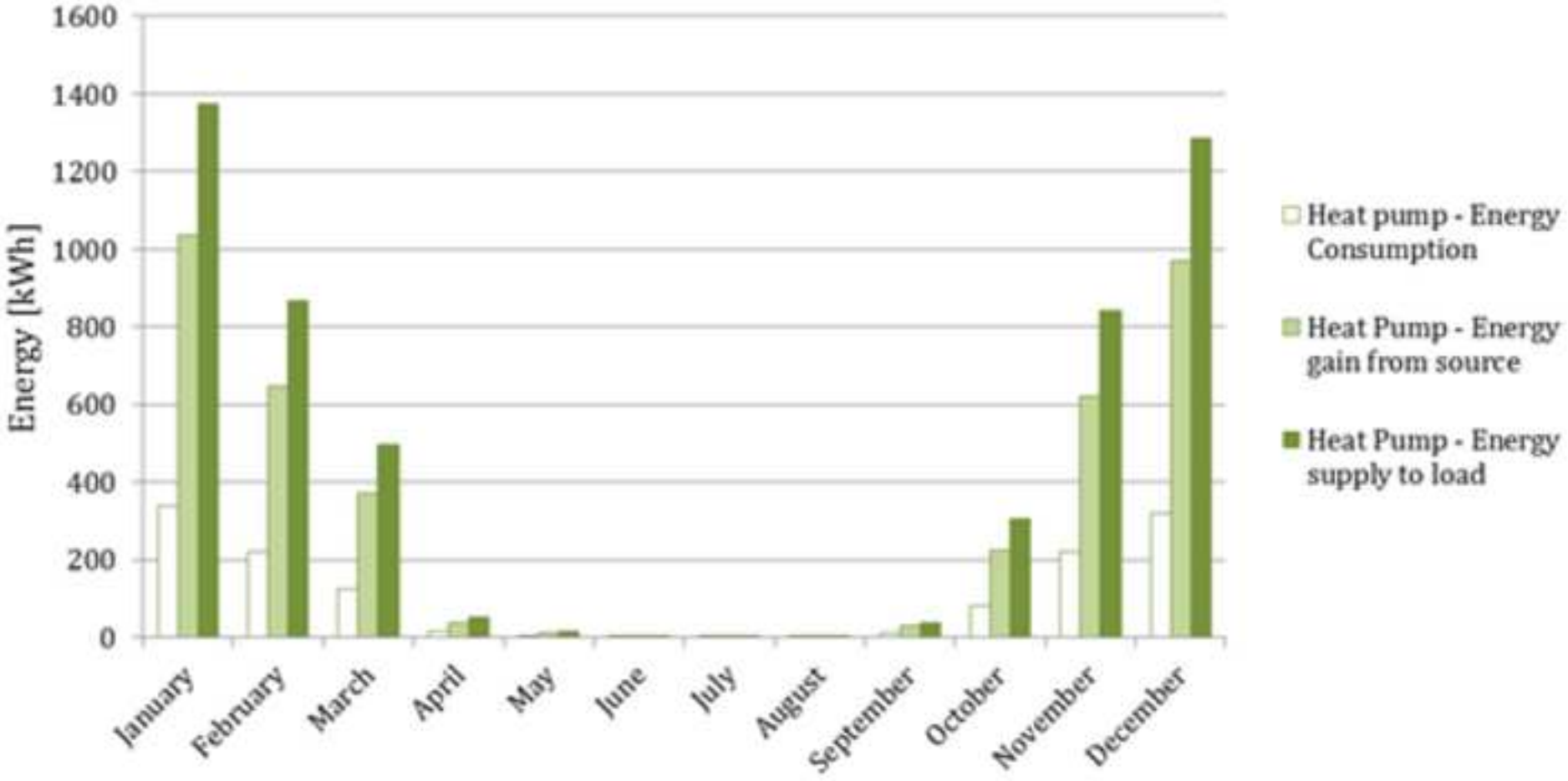

Figure 7

Click here to download high resolution image

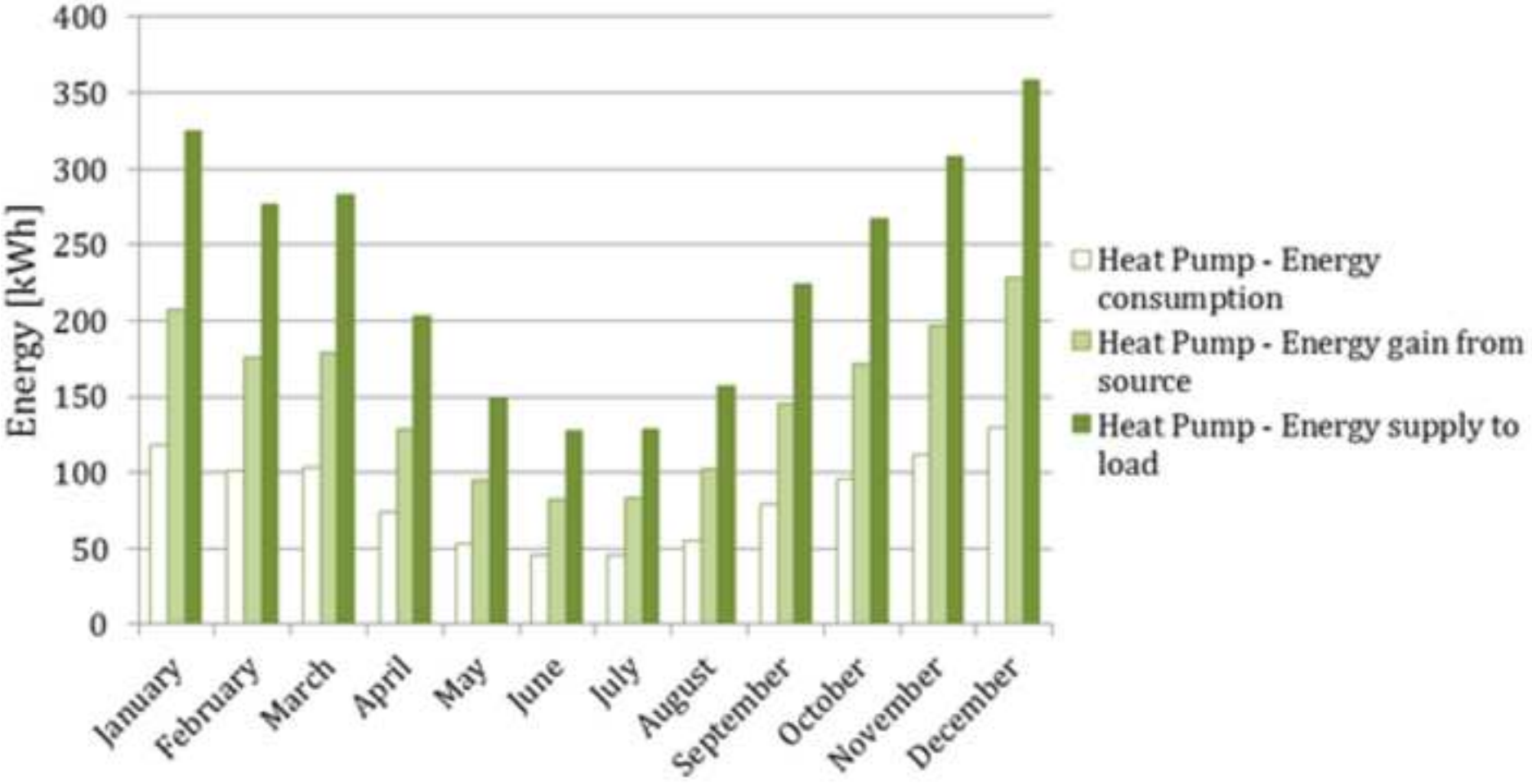

Figure 8

Click here to download high resolution image

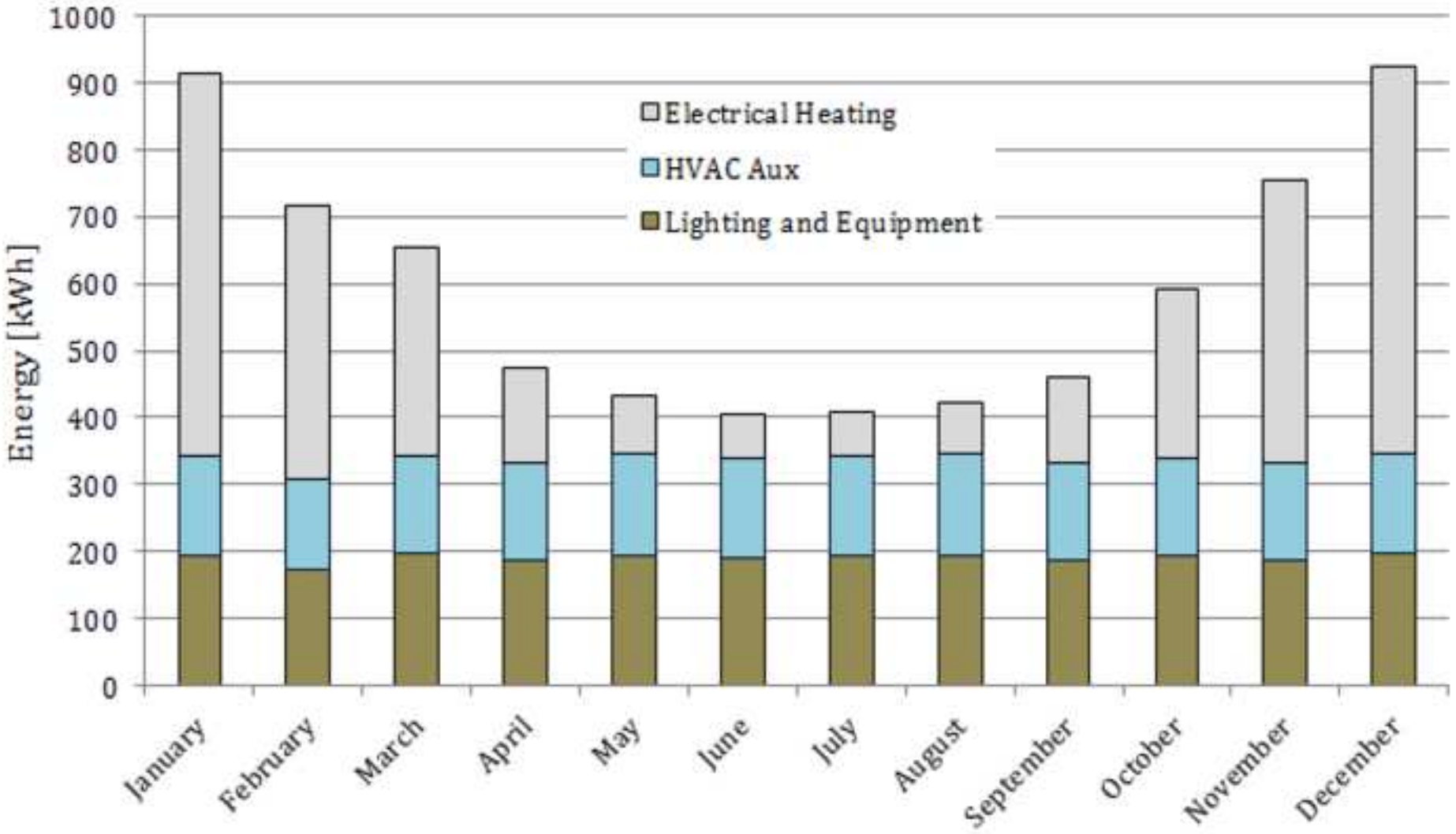

Figure 9

Click here to download high resolution image

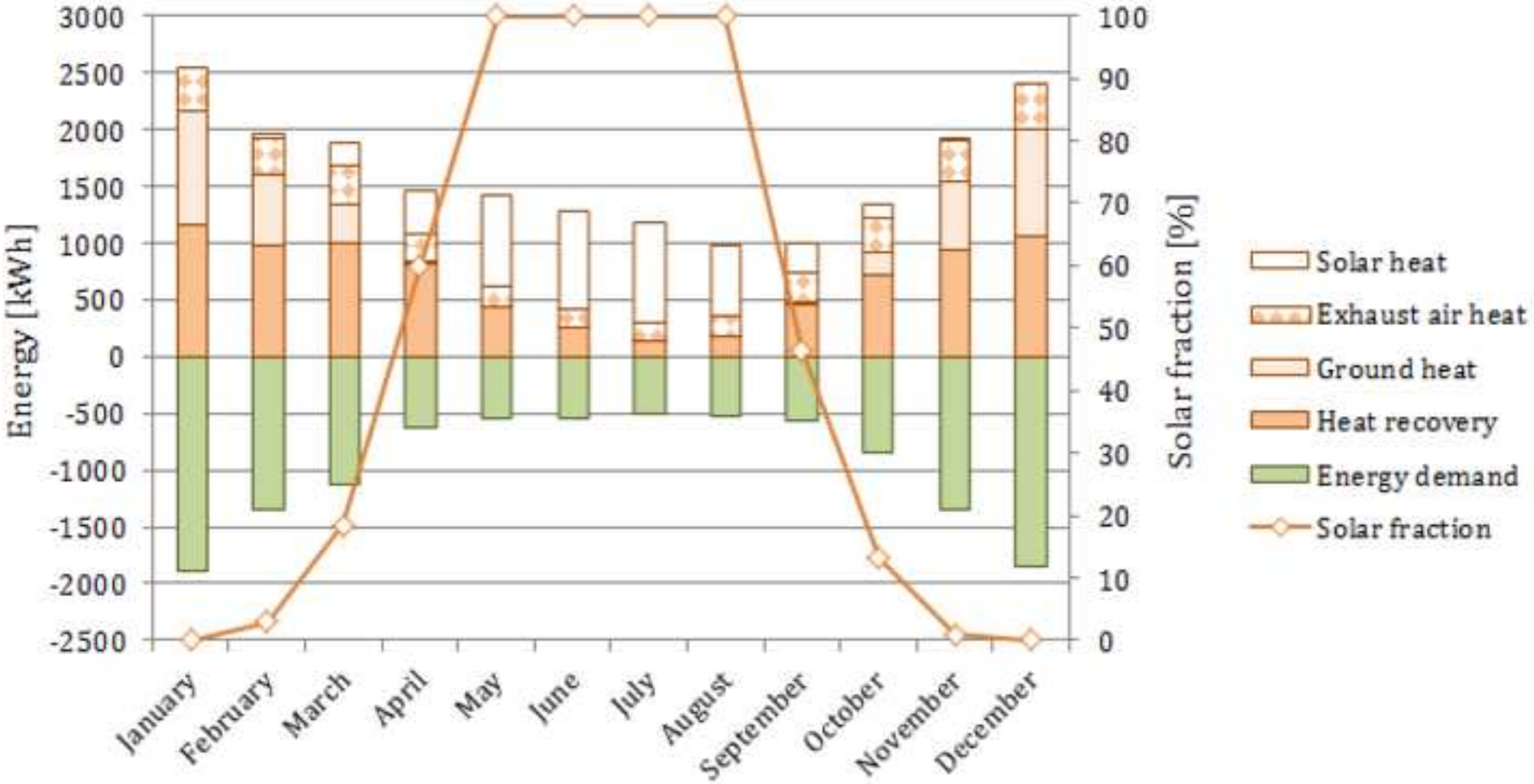

Figure 10

Click here to download high resolution image

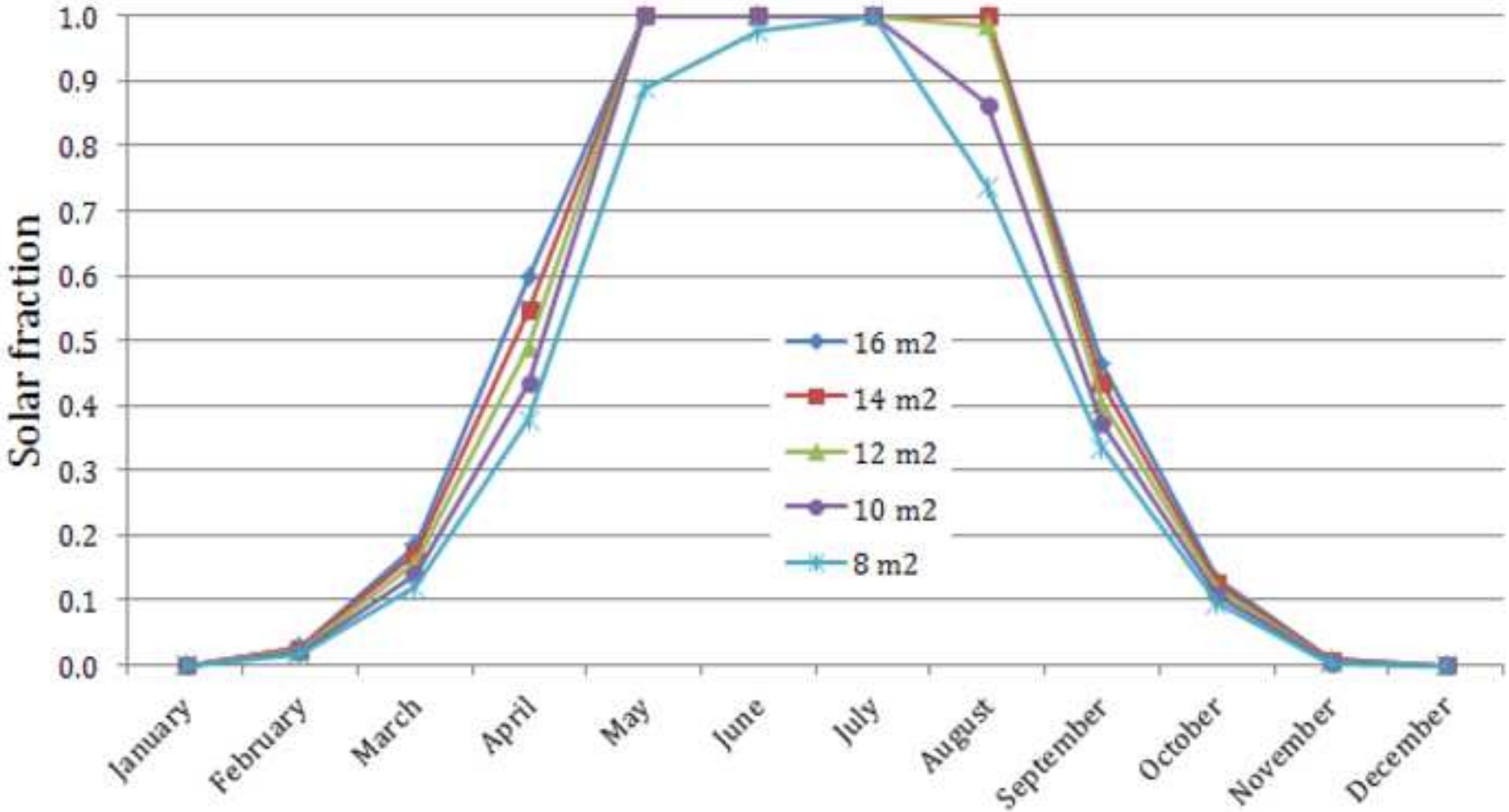

Figure 11
Click here to download high resolution image

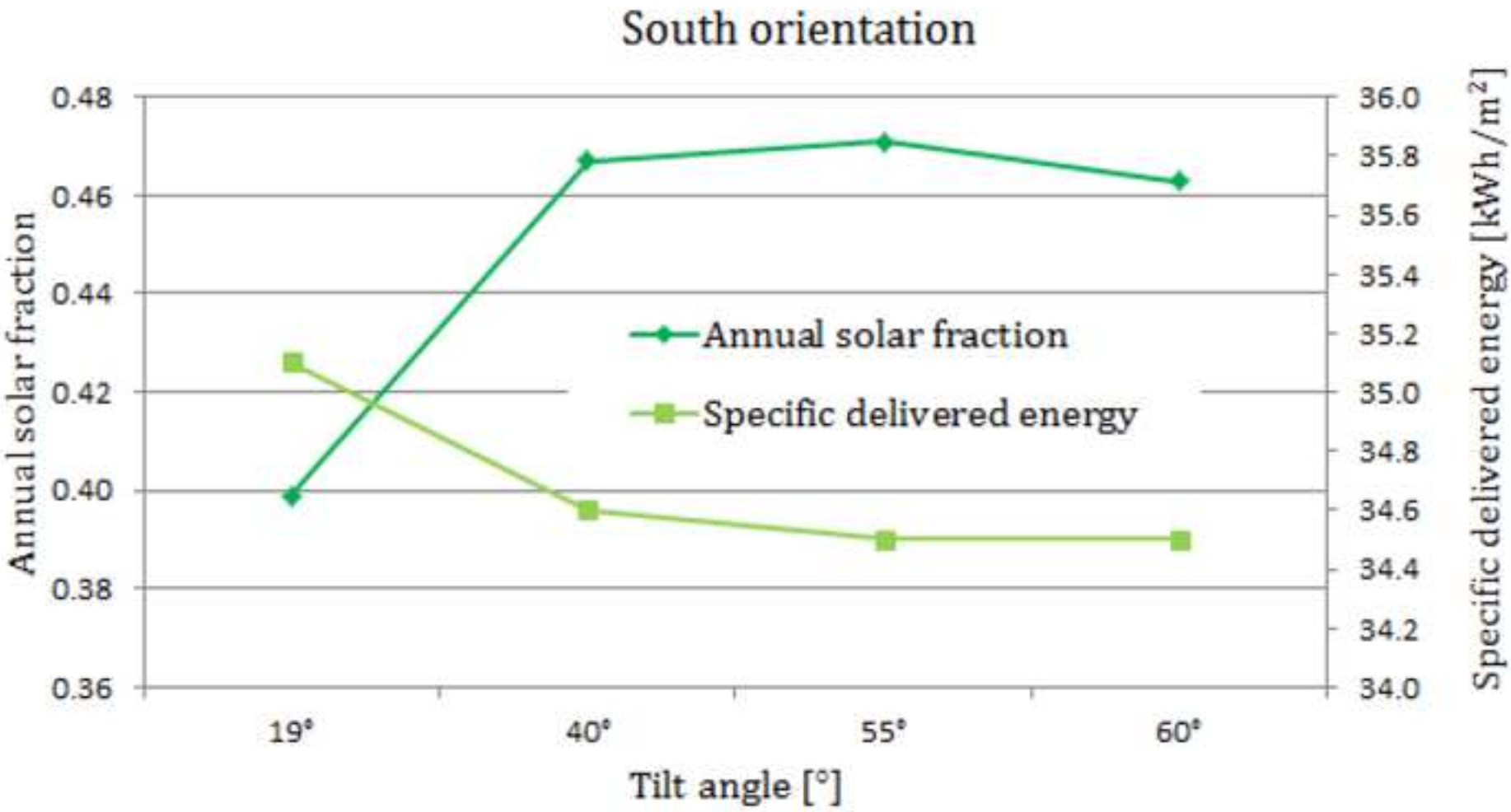

Figure 12
Click here to download high resolution image

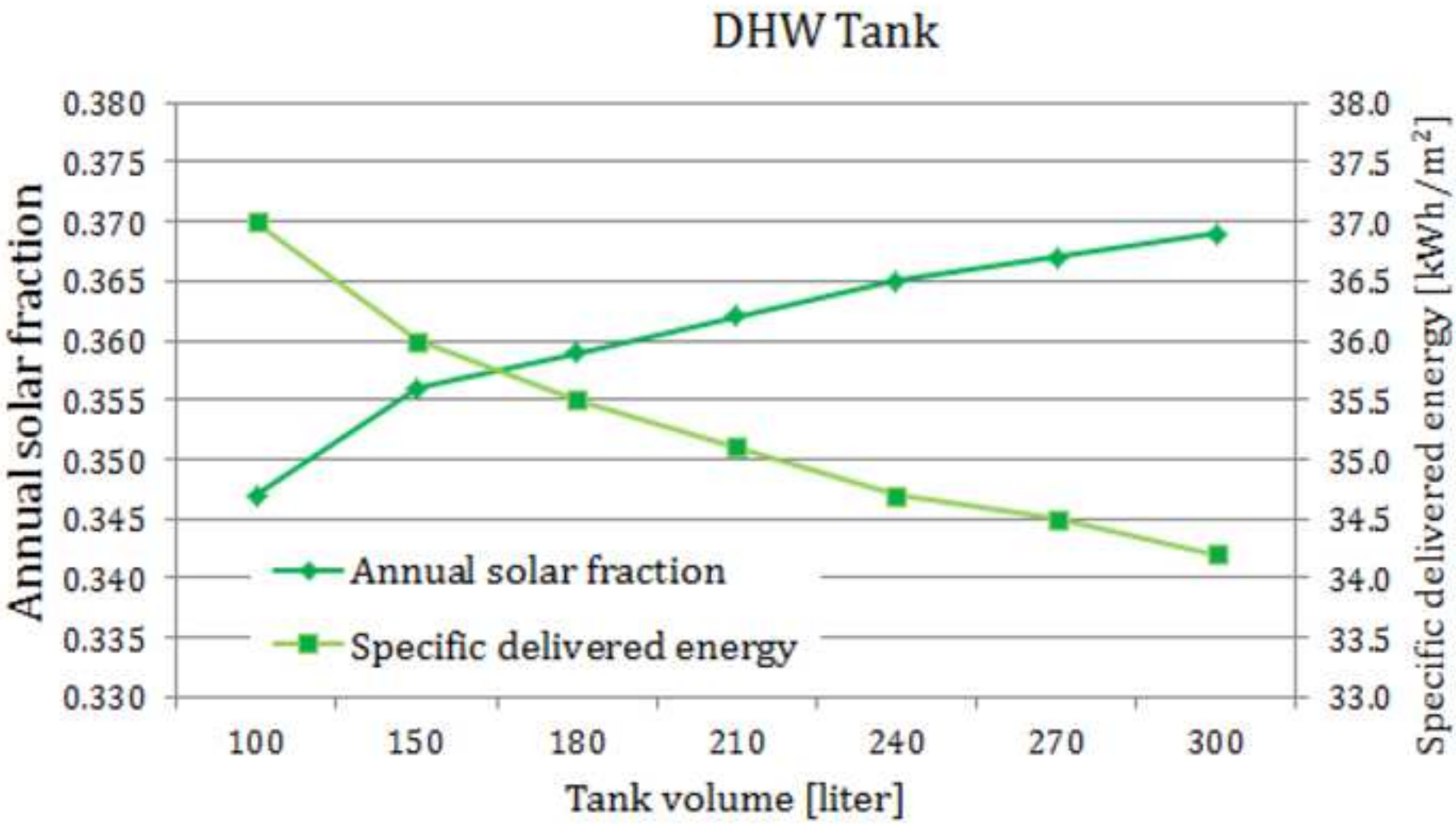

Figure 13
Click here to download high resolution image

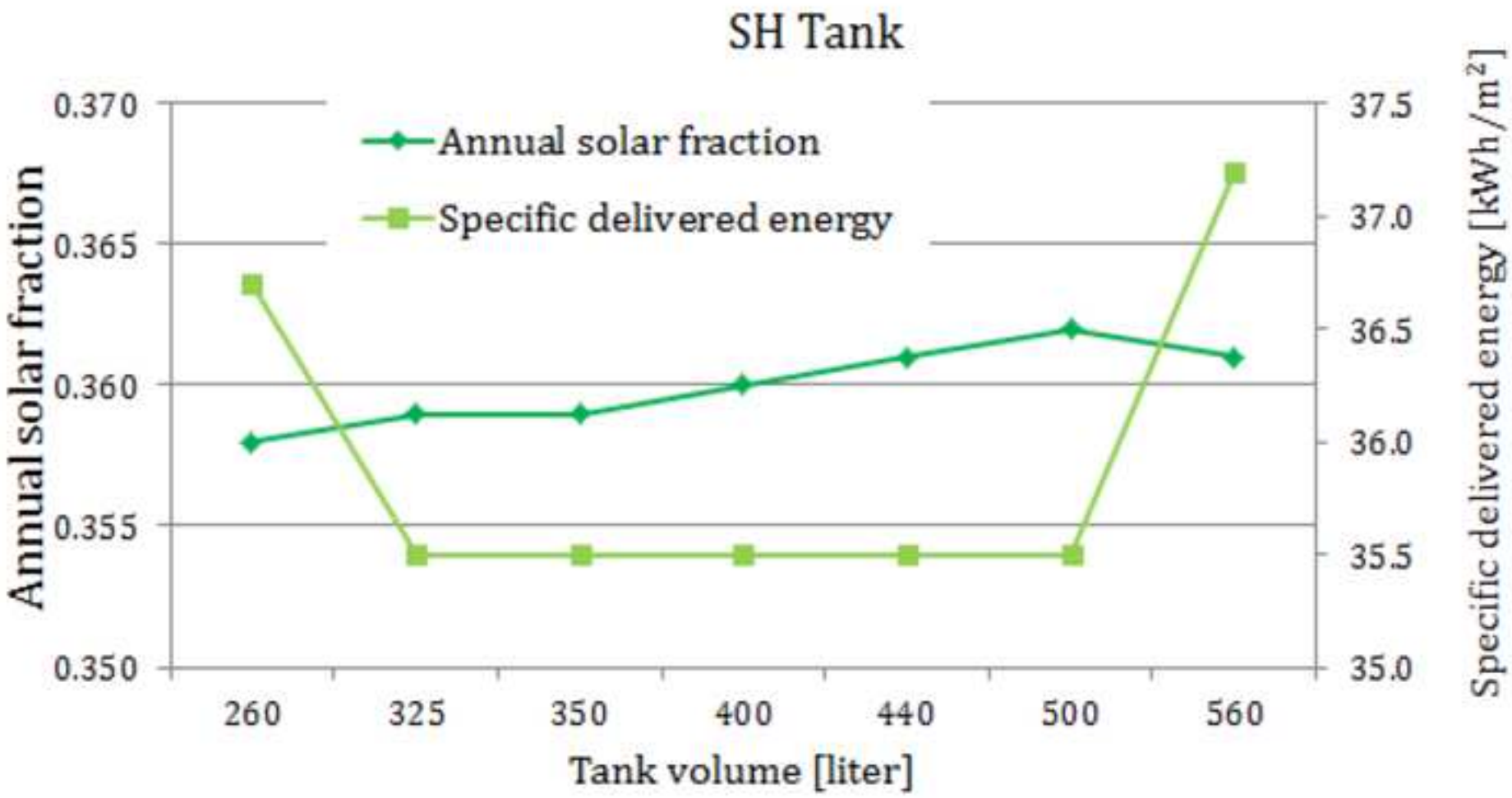

Figure 14

Click here to download high resolution image

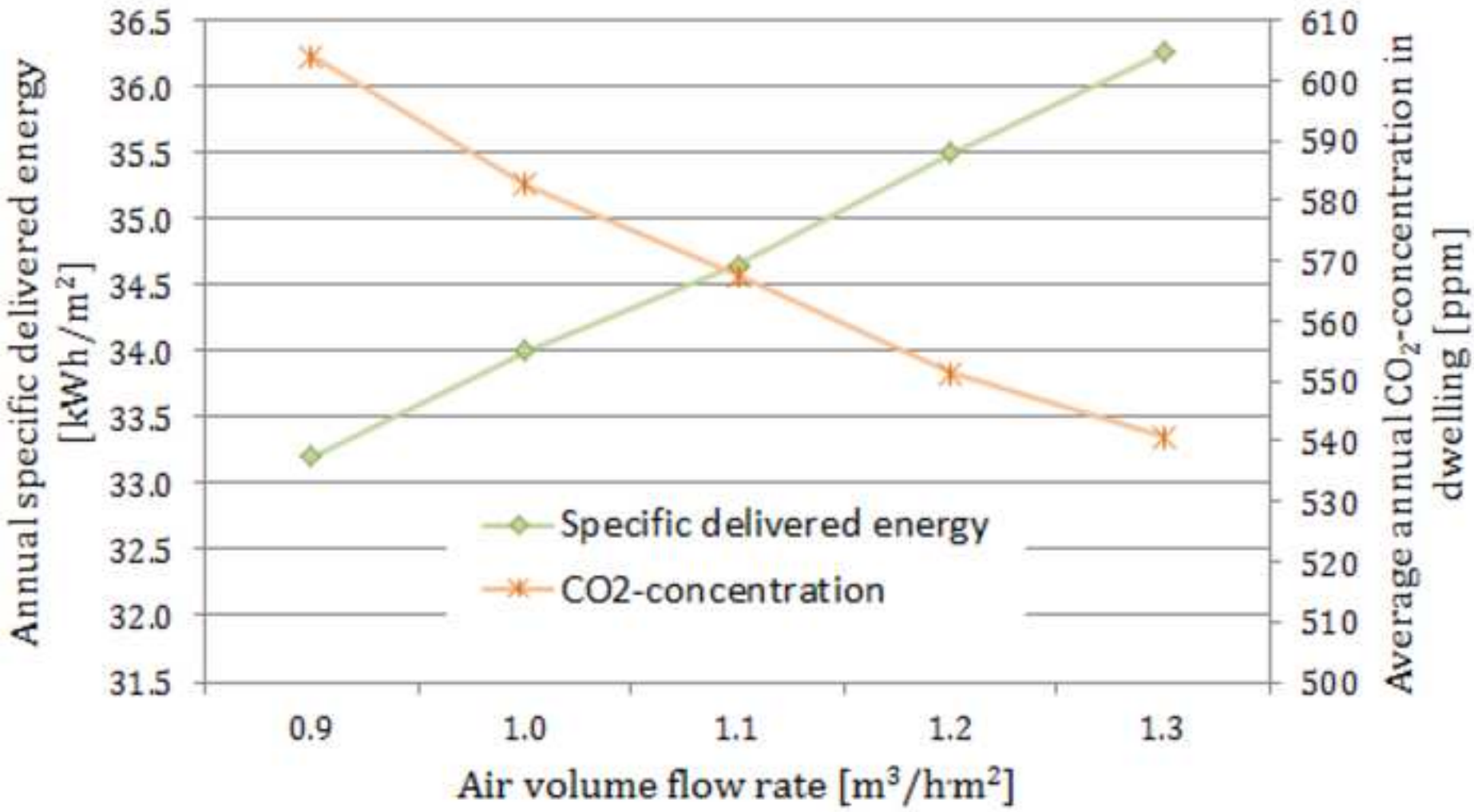

Figure 15

Click here to download high resolution image